

# Bayesian Uncertainty Assessment in Deterministic Models for Environmental Risk Assessment

Samantha Bates

Adrian Raftery

Alison Cullen



# NRCSE

Technical Report Series

NRCSE-TRS No. 058

November 13, 2000

The **NRCSE** was established in 1996 through a cooperative agreement with the United States Environmental Protection Agency which provides the Center's primary funding.



# Bayesian Uncertainty Assessment in Deterministic Models for Environmental Risk Assessment

Samantha Bates<sup>\*†</sup>, Adrian E. Raftery<sup>\*</sup> and Alison Cullen<sup>‡</sup>

## Abstract

We use Bayesian methodology to make inference from deterministic models while accounting for uncertainty in the inputs to the model. The method uses all available information, both data and expert knowledge based and extends current methods of ‘uncertainty analysis’ by updating using available data. We present an application of these methods to a deterministic model for polychlorinated biphenyl (PCB) concentration in soil. The result is a distribution of concentration in soil which accounts for uncertainty, but is not over-conservative, as the more traditional approaches can be.

**Key Words:** Deterministic Models, Bayesian Methods, Sampling Importance Resampling, Uncertainty.

## 1 Background

Risk is the probability of some adverse effect, and risk assessment is a process by which an estimate of this probability is obtained. A risk assessment generally follows four steps; hazard identification, dose-response assessment, exposure assessment and risk characterization. In the hazard identification step, the hazard (potential or real) and its adverse effects (if any) are identified. The exposure assessment step identifies populations which could be exposed and the pathways by which this may occur. The dose-response step quantifies the relationship between levels of exposure and the level of potential adverse effect (Faustman and Omenn 1996). The final risk characterization step involves combining the results of the previous three steps to determine some endpoint of interest,

---

<sup>\*</sup>Department of Statistics, University of Washington, Box 354322, Seattle, WA 98195-4322.

<sup>†</sup>Corresponding Author. Email: sam@stat.washington.edu

<sup>‡</sup>Daniel J. Evans School of Public Affairs, University of Washington, Box 353055, Seattle, WA 98195-3055.

for instance, the risk of an adverse health effect for an individual exposed to a contaminant. This paper focuses on problems in the exposure assessment phase of a risk assessment. We consider the case in which exposure to some contaminant or event is modeled by a deterministic model which relates an output (such as contaminant concentration) to a group of inputs.

Until the 1980s most literature on quantitative methods for exposure assessment concentrated on purely deterministic approaches whereby inputs to an exposure model were assigned a 'point estimate'. However, inputs to an exposure model are often not known precisely. This lack of information or lack of knowledge is often referred to in the risk assessment community as *uncertainty*. In addition to this uncertainty, there may be *variability*, natural heterogeneity in the population of interest or across time and space.

In the 1980s authors began to call for a probabilistic approach to exposure assessment to account for uncertainty and/or variability (Morgan et al. 1985; Bailey 1997; US EPA 1997b). Our aim here is to present a Bayesian method which accounts for the uncertainty about the values of model inputs and propagates this through the model to the output. This will be done by using all available information, both subjective and application-specific empirical data. The result will be a distribution for an endpoint of interest which accounts for uncertainty and which decision-makers could use to set conservative bounds.

## 2 Approach

Suppose we have a deterministic simulation model  $M$  which maps inputs  $\theta$  to outputs  $\phi$ . The quantities  $\theta$  and/or  $\phi$  may be single or vector valued. We refer to  $M(\theta)$  as the induced output, i.e. the value of the output that is induced by the model from the input  $\theta$ . Further, suppose that the available expert knowledge about the values of the inputs is represented by a prior distribution, which we denote by  $p(\theta)$ .

Often in environmental risk assessments, the collection of data specific to the assessment at hand is expensive, and so such data tend to be sparse. We would like a method which uses all available information on the model inputs and outputs, including the sparse and expensive data, to make inference from the model. This observed data can be used to form likelihoods for  $\theta$  and  $\phi$  which are denoted respectively by  $L_{inp}(\theta)$  and  $L_{out}(\phi)$ . The existence of either likelihood is not essential.

Let  $D$  denote the observed data. The marginal posterior distribution of the inputs,  $\pi^{[\theta]}(\theta)$ , is the conditional distribution of  $\theta$  given both  $D$  and the model  $M$ . Suppose we can partition  $D$  into components relating to  $\theta$  and  $\phi$  respectively:  $\{D_\theta, D_\phi\}$ . Then, by Bayes's theorem:

$$\begin{aligned}\pi^{[\theta]}(\theta) &\propto P(\theta | M) P(\{D_\theta, D_\phi\} | \theta, M) \\ &= p(\theta) L_{inp}(\theta) L_{out}(M(\theta)).\end{aligned}\tag{1}$$

Thus  $\pi^{[\theta]}(\theta)$  is proportional to the product of three factors: the prior on the inputs, the likelihood of the inputs, and the likelihood of the outputs evaluated at the induced values.

Inference about  $\phi$ , or any function of it, can be made from its marginal posterior distribution, the distribution of  $\phi = M(\theta)$  when  $\theta \sim \pi^{[\theta]}(\theta)$ . Thus we need a method to find  $\pi^{[\theta]}(\theta)$ . Often, the analytical form of  $\pi^{[\theta]}(\theta)$  is intractable and obtaining an exact sample from it can be difficult or impossible. One method to obtain an approximate sample from  $\pi^{[\theta]}(\theta)$  is to use the sampling importance resampling (SIR) algorithm of Rubin (1988). This algorithm involves initially sampling from a known distribution and resampling according to SIR weights.

When, as in our application, the prior is easily sampled from, each SIR weight is the ratio of  $\pi^{[\theta]}(\theta)$  and  $p(\theta)$  for a value of  $\theta$  sampled from the prior. Let  $\theta_i$  denote the  $i^{th}$  sample from the prior on the inputs,  $p(\theta)$ , with corresponding induced value  $\phi_i = M(\theta_i)$ . Using the relation in (1), the SIR weight associated with  $\theta_i$  and  $\phi_i$  is

$$w_i = \frac{\pi^{[\theta]}(\theta_i)}{p(\theta_i)} \propto L_{inp}(\theta_i) L_{out}(M(\theta_i))\tag{2}$$

More details on the use of the SIR algorithm in this context can be found in Poole and Raftery (2000).

### 3 Application: Soil Concentration of PCBs

A severely contaminated region of New Bedford Harbor, MA (NBH) was designated as a Superfund site in 1982 due to a high concentration of polychlorinated biphenyls (PCBs), a probable human carcinogen (US EPA 1997a). The PCBs were introduced to the harbor in waste dumped between the 1940s and the late 1970s by local industry. PCBs in contaminated sediment or water can travel to other media, such as air, soil or food. PCBs may also be present in old household electrical appliances. Dredging of the hotspot began in 1994 and proceeded as part of a cleanup. Dredging occurs at low tide and disturbs the contaminated sediment which may increase the transport of PCBs to air via volatilization.

Table 1: Description of Inputs to Model (3).

<b>Input</b>	<b>Description</b>	<b>Unit</b>
$Ca$	PCB concentration in air.	$mg/m^3$
$Vd$	Deposition velocity.	$m/d$
$b$	Decay constant in soil.	$1/d$
$\rho$	Density of the soil.	$g/m^3$
$D$	Mixing depth of soil.	$m$

In order to estimate the additional risk of cancer due to exposure to PCBs in a year, one requires an estimate of the average level of PCB a person could be exposed to in a year. For people with no occupational exposure to PCBs, indirect exposure pathways such as contaminated soil, dust or food may contribute significantly to overall exposure. An important intermediate step in determining the level of exposure through indirect pathways is estimating the average concentration of PCB in soil due to one year of exposure.

Taylor (1992) adapted a deterministic single compartment steady-state model for predicting contaminant concentration in soil from the concentration in air from its original form in Fries and Paustenbach (1990). The model has a single output,  $Cs$ , the contaminant concentration in soil ( $mg/g$ ), and five inputs, and is given by:

$$Cs = \frac{Ca Vd}{b \rho D}. \quad (3)$$

Descriptions of the inputs are given in Table 1. The numerator in (3) represents the mass flux (deposition) of the contaminant from air onto soil. The denominator represents the dilution or decay of the contaminant in the soil (Cullen 2000).

Researchers have measured PCB concentration in 19 air and 18 soil samples taken from a site upwind of the harbor in Dartmouth, MA. The method of data collection and protocols followed are described in Vorhees, Cullen, et al. (1997) and Vorhees, Cullen, et al. (1999). PCB concentrations in these upwind samples do not reflect dredging induced fluxes related to the NBH cleanup which would invalidate the use of a steady-state model.

Hereafter PCB concentration refers to the sum of the 59 prevalent, persistent and toxic PCB congeners for which the samples were analyzed. Individual congener information can be obtained from Table 2 of Cullen et al. (1996).

### 3.1 Model Specification

Taking an expectation of the log of (3) with respect to space and time we find

$$\mu_{\ln(Cs)} = \mu_{\ln(Ca)} + \ln\left(\frac{Vd}{b\rho D}\right)$$

where  $\mu_{\ln(Cs)}$  and  $\mu_{\ln(Ca)}$  are the mean of logged average soil and air PCB concentrations respectively. Soil PCB concentration has spatial but no temporal dependence under (3) due to the steady state assumption. The PCB concentration in air varies over both space and time. Thus  $\ln(Ca)$  has an extra component of variability which needs to be accounted for.

Assuming additivity on the log scale we can decompose the variability in soil and air PCB concentration into a spatial component, a measurement error component and an additional temporal component for air concentration. Then,

$$\sigma_{\ln(Cs)}^2 = V_s^S + \gamma^S \quad \text{and} \quad \sigma_{\ln(Ca)}^2 = V_s^A + V_t^A + \gamma^A$$

where  $\sigma_{\ln(Cs)}^2$  and  $\sigma_{\ln(Ca)}^2$  represent the total variability in  $\ln(Cs)$  and  $\ln(Ca)$  respectively,  $V_s^S$  and  $V_s^A$  are the spatial components for soil and air,  $V_t^A$  is the temporal component for air, and  $\gamma^S$  and  $\gamma^A$  are the measurement error components.

In terms of the formulation in Section 2 we have,

$$\begin{aligned} \text{Inputs:} \quad \boldsymbol{\theta} &= \left( \ln(b), \ln(\rho), \ln(D), \ln(Vd), \mu_{\ln(Ca)}, \sigma_{\ln(Ca)}, V_s^S, V_s^A, \gamma^A, \gamma^S \right) \\ \text{Outputs:} \quad \boldsymbol{\phi} &= \left( \mu_{\ln(Cs)}, \sigma_{\ln(Cs)} \right) \\ \text{Model:} \quad M &: \left( \begin{array}{l} \mu_{\ln(Cs)} = \mu_{\ln(Ca)} + \ln\left(\frac{Vd}{b\rho D}\right) \\ \sigma_{\ln(Cs)}^2 = V_s^S + \gamma^S \end{array} \right) \end{aligned} \quad (4)$$

Note that

$$V_t^A = \sigma_{\ln(Ca)}^2 - V_s^A - \gamma^A \quad (5)$$

is an intermediate output.

### 3.2 Priors and Likelihoods

Priors for  $b, \rho$  and  $D$  were given in Cullen (1995) in an analysis of human exposure to emissions from waste incinerators. These priors were based on appropriate available literature and expert knowledge to adapt them to the site in question. They are applicable also to the NBH site.

Table 2 details the priors placed on each input.

In Cullen (1995), deposition velocity was initially assigned a mixture of 13 log-uniform distributions reflecting dependence of the velocity at which a contaminant falls to the ground on the size of particle that it adheres to or whether it occurs as a vapor. However it is believed that the behavior of larger particles is well described by Stokes Law while the settling of smaller particles is most effectively described by Brownian motion (Sehmel 1980). Using this reasoning and the results of Cullen’s analysis, several of the particle classes were later pooled. We follow her pooled approach and assign as a prior to deposition velocity a mixture of three log-uniform densities corresponding to fine (0.1-1.0  $\mu m$ ) and coarse (1-10 $\mu m$ ) particles and a vapor phase<sup>1</sup>.

Let  $\mathbf{p} = (p_c, p_f, p_v)$  be the proportion of total PCB adhered to coarse and fine particles or occurring as a vapor, respectively. A Dirichlet prior was assigned to  $\mathbf{p}$  that was consistent with the following ranges for the marginal distributions,  $p_c \in [0.0085, 0.13]$ ,  $p_f \in [0.0015, 0.03]$ ,  $p_v \in [0.85, 0.99]$ . Experimental measurements on which to base these ranges are only estimates due to difficulties in sampling a large enough volume of air and hence PCB in a sampling period. From Falconer and Bidleman (1994) we derived the proportion of individual congeners adhered to either coarse or fine particles in air of 10 deg C (50F) and 25 deg C (77F). Ranges for  $p_c + p_f$  and  $p_v$  for total PCB were derived from these results by using the relative loadings of the individual congeners found in the NBH samples (Vorhees, Cullen, et al. 1997) and by considering both air temperatures. Steinberg, Reckhow, et al. (1995) also considered relative loadings in deriving priors. Whitby (1978) reports that approximately 15% of the volume of background average air is in fine particles, this was used to separate the ranges for  $p_c$  and  $p_f$ .

Vorhees, Cullen, et al. (1997) reported that measured air and soil PCB concentrations were  $\pm 10\%$  (as assessed in blanks). Assuming a normal distribution on the logged errors, the measurement error variances  $\gamma^A$  and  $\gamma^S$  were both set equal to 0.0025.

We use unit information priors for  $V_s^A$  and  $V_s^S$ . Such priors are proper, but diffuse relative to the likelihood, and hence tend to have little effect on inference (Kass and Wasserman 1995; Raftery 1999). The spatial variability in soil should be greater than that in air. Hence we impose the condition that  $V_s^S > V_s^A$  as part of the prior specification. Due to this dependence of  $V_s^S$  on  $V_s^A$ , the intermediate output  $V_t^A$  given in (5) now plays a role in the calculation of the output  $\sigma_{\ln(C_s)}$ .  $V_t^A$  represents the temporal component to variability in air PCB concentration and must be non-negative. This introduces constraints on the priors for both  $\sigma_{\ln(C_a)}$  and  $V_s^A$ .

---

<sup>1</sup>1 million  $\mu m = 1$  meter

Table 2: Priors on Inputs

Input	Prior	Note
$b$	Uniform(0.0001, 0.0002)	
$\rho$	Log <sub>e</sub> Normal( $1.4 \times 10^6$ , 1.15)	1
$D$	Uniform(0.15, 0.25)	
$Vd$ for:		
Coarse Particles	Log <sub>10</sub> Uniform(10, 1000)	2
Fine Particles	Log <sub>10</sub> Uniform(1, 100)	2
Vapor Phase	Log <sub>10</sub> Uniform(10, 1000)	2
$\mathbf{p}$	Dirichlet( $20 \times (0.06, 0.01, 0.9)$ )	
$\mu_a$	Normal( $-14.73$ , 1.54)	
$\sigma_a^2$	Scaled Inv- $\chi_1^2(1.54) \mid V_t^A \geq 0$	3
$V_s^A$	Scaled Inv- $\chi_1^2(0.0024) \mid V_t^A \geq 0$	3
$V_s^S$	Scaled Inv- $\chi_1^2(0.0064) \mid (V_s^S > V_s^A)$	3
$\gamma^A, \gamma^S$	0.0025	

1. If  $X \sim \text{Log}_e \text{Normal}(a, b)$  then  $\ln(X) \sim \text{Normal}(\ln(a), b^2)$ .
2. If  $X \sim \text{Log}_{10} \text{Uniform}(a, b)$  then  $\log_{10}(X) \sim \text{Uniform}(\log_{10}(a), \log_{10}(b))$ .
3. If  $X \sim \text{Scaled Inv-}\chi_a^2(b)$  then  $X$  has an inverse  $\chi^2$  density with  $a$  df and scaled by  $b$ .

The observed PCB concentrations in air are 24 hour average measurements. The inputs  $\mu_{\ln(Ca)}$  and  $\sigma_{\ln(Ca)}$  are the mean and standard deviation of annual average air PCB concentration. This disparity in time scale has to be accounted for.

Let  $\mu_a$  and  $\sigma_a$  be the mean and standard deviation of 24 hour average logged air PCB concentration.  $\mu_a$  and  $\sigma_a$  are given diffuse unit information priors estimated using the observed (24 hour average) concentrations. The form of each prior represents the information that a single observation would provide and are given in Table 2.

Pollutant concentrations are believed to follow a log-normal distribution. Ott (1990) justified this distribution in the general case using a dilution argument with the central limit theorem to show that the product of independent random variables has a log-normal distribution.



Assuming that the observed air data are i.i.d., the likelihood for the observed air data given the inputs is:

$$L_{inp}(\boldsymbol{\theta}) = \prod_{i=1}^{19} N\left(Y_i^A; \mu_a, \sigma_a^2\right)$$

where  $Y_i^A$  is the  $i^{th}$  logged observed 24 hour average air measurement.

In the NBH region, weather is believed to occur in five day cycles (Cullen and Frey 1999). It follows that there are approximately 73 of these cycles in a year. We follow Cullen and Frey (1999) in assuming that the expected annual average air concentration equals the expected 24 hour average air concentration but variability in annual average is the variability in 24 hour average concentration reduced by a factor of 73. Under these assumptions and using properties of the log-normal distribution, the 24 hour average values can be converted to the annual average parameters  $\mu_{ln(Ca)}$  and  $\sigma_{ln(Ca)}$  and these used in model (4). The formulae for this conversion are given by (6) and (7).

$$\mu_{ln(Ca)} = \mu_a + 0.5 \sigma_a^2 - 0.5 \ln\left(1 + \frac{e^{\sigma_a^2} - 1}{73}\right) \quad (6)$$

$$\sigma_{ln(Ca)}^2 = \ln\left(1 + \frac{e^{\sigma_a^2} - 1}{73}\right) \quad (7)$$

The observed PCB concentrations in soil reflect long-term averaging. The outputs,  $\mu_{ln(Cs)}$  and  $\sigma_{ln(Cs)}$  are on this long-term scale also. Assuming that the observed soil data are i.i.d., the likelihood for the observed soil data given the outputs and model is:

$$L_{out}(\boldsymbol{\phi}) = \prod_{i=1}^{18} N\left(Y_i^S; \mu_{ln(Cs)}, \sigma_{ln(Cs)}^2\right)$$

where  $Y_i^S$  is the  $i^{th}$  logged observed soil measurement.

The assumption that the observed data are independent may not be correct, but the data are too few to provide evidence of spatial or temporal dependence, or of the form that it would take. Our modeling of the variation in air concentration in terms of five-day cycles is an effort to take account of temporal autocorrelation.

### 3.3 Results

Unless previously stated, prior independence of the inputs was assumed. An initial sample of size 50,000 was generated from the priors in the first step of the SIR algorithm, and in the resampling step of the SIR algorithm, a sample of size 5,000 was used. This produced just over 1,000 unique values in the marginal posterior distributions for each element of  $\boldsymbol{\theta}$  and  $\boldsymbol{\phi}$ . This was enough to provide a reasonable estimate of the posterior distributions of interest.

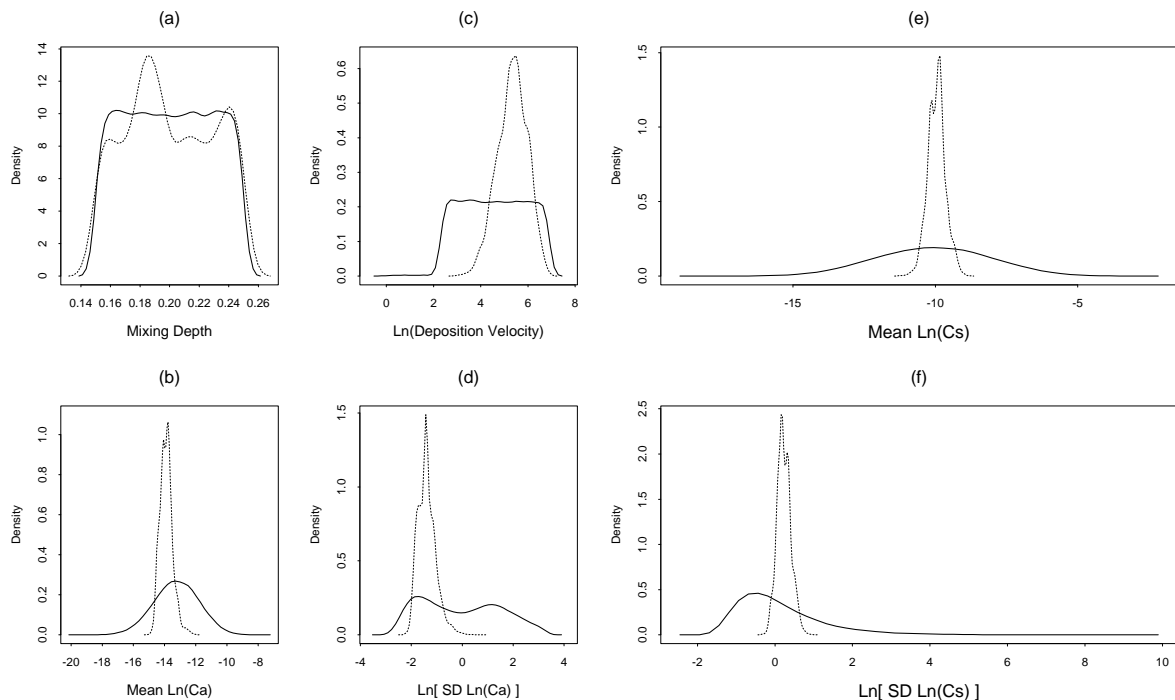


Figure 1: (a)-(d): Nonparametric density estimates of prior (solid line) and posterior distributions (dotted) for selected model inputs;  $D$ ,  $V_d$  and the air parameters. (e)-(f): Nonparametric density estimates of induced (solid) and posterior distributions (dotted) for the model outputs.

Figure 1(a)-(d) shows estimates of the posterior distributions of mixing depth, deposition velocity and the parameters of the distribution for  $\ln(Ca)$ , based on the sampled values. These were calculated by nonparametric kernel density estimation from the set of sampled values. These are overlaid on estimates of the prior densities. Both Monte Carlo variability and edge effects are evident in the estimates. Inspection of these plots can reveal whether the observed data in the form of likelihoods provided much information on the inputs or outputs.

The posterior distribution of mixing depth shows little updating over the prior, suggesting that the observed data did not contain much additional information. There is a large amount of updating in Figure 1(c). This suggests that under this model the observed data are consistent with faster deposition velocities. This corresponds to PCB adhering to coarse particles or occurring in the vapor phase, rather than adhering to fine particles. The inputs  $\mu_{\ln(Ca)}$  and  $\sigma_{\ln(Ca)}$  were given diffuse priors, so a large amount of updating was expected and is observed. Lower values of variability in air are favored by the data and the model.

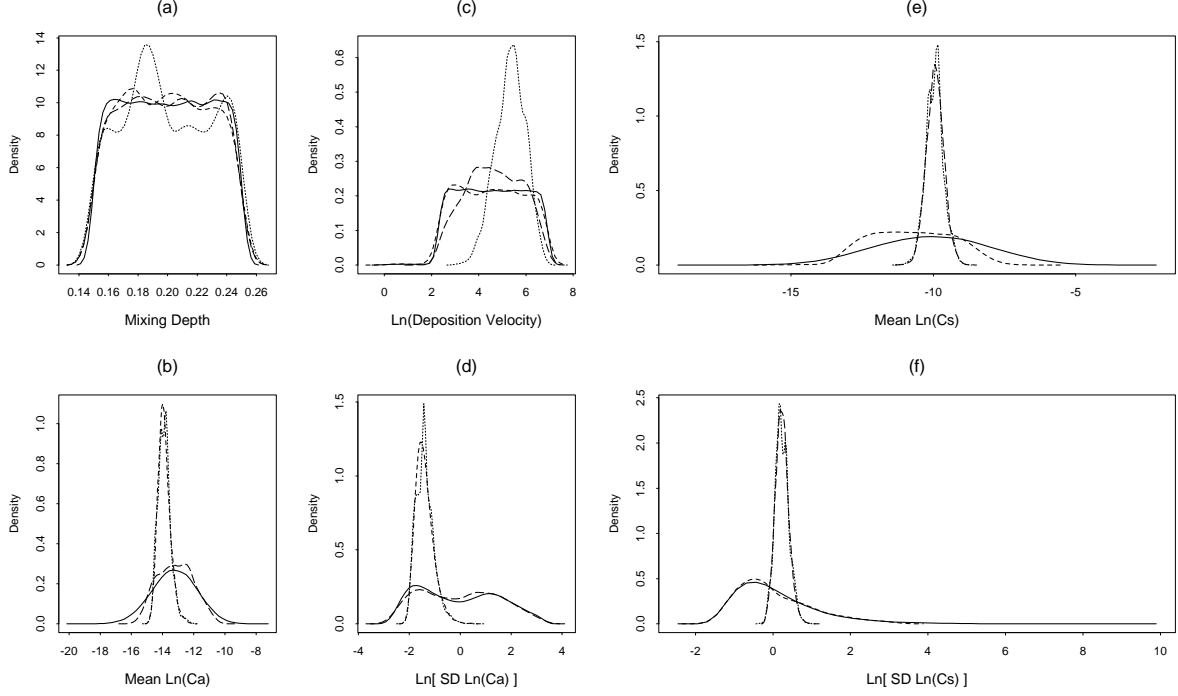


Figure 2: (a)-(d): Nonparametric density estimates of prior (solid line) and posterior distributions for selected model inputs;  $D$ ,  $Vd$  and the air parameters. (e)-(f): Nonparametric density estimates of induced (solid) and posterior distributions for the model outputs. Posterior distributions using all data (dotted line), only air data (short dashes) and only soil data (long dashes) are shown.

Figure 1(e)-(f) shows estimates of the induced and posterior distributions for the outputs  $\mu_{ln(Cs)}$  and  $\sigma_{ln(Cs)}$ . Again we expect, and observe, a large amount of updating due to the effect of diffuse priors on the induced distributions.

The posteriors just discussed represented the additional information on  $\theta$  and  $\phi$  provided by the combined effect of the two likelihoods  $L_{inp}(\theta)$  and  $L_{out}(\phi)$ . Our uncertainty about the true values of the inputs and outputs was reduced in most cases by this additional information. We may be interested in knowing which set of data is providing the information i.e. which set is reducing our uncertainty for a particular input or output?

The effect of the air data alone can be seen by examining the posterior distributions based on only the air likelihood. The SIR algorithm proceeds as before, but in this case the resampling is performed with weights dependent on only  $L_{inp}(\theta)$ . The SIR weight associated with  $\theta_i$  and  $\phi_i$

is then  $w_i \propto L_{inp}(\theta_i)$  rather than those given in (2). A similar approach is used to examine the relative effect of the soil data alone.

The plots given in Figure 2(a)-(d) show that it is the air data which contain the most information on the air parameters. This is because the posterior based on only the soil data shows no update over the prior distribution. Neither data set contains information on mixing depth and it is the soil data that are consistent with the faster deposition velocities. In Figure 2(e)-(f) it is the soil data that reduce the uncertainty about the soil parameters  $\mu_{ln(Cs)}, \sigma_{ln(Cs)}$ .

### 3.4 Sensitivity Analysis

Given the unusual behavior indicated by the posterior distribution for deposition velocity, we investigated the sensitivity of  $Vd$  and  $\phi$  to changes in the priors placed on the mixing proportions  $\mathbf{p}$ . Table 3 shows results of halving and doubling the variability in the marginal distribution of each mixing proportion while retaining the means. We then show results with equal means while retaining the original variance. Perturbation of the Dirichlet parameters for  $\mathbf{p}$  resulted in changes in the posterior mean, standard deviation and median which were within Monte Carlo variability.

Table 3: Sensitivity analysis results for  $\phi$  and  $Vd$  to changes in the prior for  $\mathbf{p}$ . Posterior mean, median and standard deviation (SD) for  $Vd$ ,  $\mu_{ln(Cs)}$  and  $\sigma_{ln(Cs)}$  based on the original simulation where  $\mathbf{p} \sim \text{Dirichlet}(\alpha_0 = (1.2, 0.2, 18))$  are given in the first row. Subsequent values are the percentage change resulting from the perturbation of the original Dirichlet parameters.

Dirichlet Parameters	$Vd$			$\mu_{ln(Cs)}$	$\sigma_{ln(Cs)}$
	Median	Mean (SD)		Mean (SD)	Mean (SD)
$\alpha_0$	212.77	249.64	(152.92)	-9.959 (0.307)	1.283 (0.234)
$\alpha$ such that $\text{Var}(p_i)$ is halved	5.3%	-1.1%	(-8.8%)	0.2% (1.6%)	-0.5% (-5.1%)
$\alpha$ such that $\text{Var}(p_i)$ is doubled	3.4%	-1.4%	(-8.7%)	0.1% (5.2%)	-0.3% (0.4%)
$\alpha$ such that $E(p_c)=E(p_f)=E(p_v)$	-9.5%	-7.3%	(-10.1%)	0.0% (-2.8%)	-0.9% (-5.1%)

Table 4 gives the largest percentage change in the posterior mean and standard deviation for  $\mu_{ln(Cs)}$  and  $\sigma_{ln(Cs)}$  resulting from 10% increases or decreases in the parameters of each prior

distribution. All of the differences observed were within Monte Carlo variation, with the exception of those on  $\mu_{ln(Cs)}$  resulting from perturbations in the prior median for  $\rho$ .

Table 4: Sensitivity analysis results for  $\phi$ . Posterior mean and standard deviation (SD) for  $\mu_{ln(Cs)}$  and  $\sigma_{ln(Cs)}$  based on the original simulation are given in the first row. Subsequent values are the maximum absolute percentage change resulting from  $\pm 10\%$  changes in the original input prior distribution parameters.

<b>Perturbed</b>	$\mu_{ln(Cs)}$	$\sigma_{ln(Cs)}$
<b>Input</b>	<b>Mean (SD)</b>	<b>Mean (SD)</b>
Original	-9.959 (0.307)	1.283 (0.234)
$b$	0.1% (2.4%)	0.5% (1.2%)
$D$	0.1% (2.4%)	0.5% (1.2%)
Median of $\rho$	0.9% (8.6%)	0.9% (6.2%)
GSD of $\rho$	0.1% (0.5%)	0.2% (0.7%)
$\mu_a$	0.4% (4.6%)	0.9% (7.3%)
$\sigma_a$	0.0% (1.5%)	0.4% (2.7%)

### 3.5 Comparison to Other Methods

Monte Carlo, Bayesian and other probabilistic methods are relatively new in environmental risk assessment. Point estimates have traditionally been used to estimate the inputs and outputs of a deterministic model. A Monte Carlo (MC) approach pushes values of the inputs simulated from the prior distribution through the model, resulting in a distribution for the model outputs. The distribution for  $\phi = (\mu_{ln(Cs)}, \sigma_{ln(Cs)})$  developed under an MC approach is equivalent to the distribution of induced values obtained in the SIR algorithm. The main difference between an MC approach and the Bayesian one described here is that the Monte Carlo approach does not take account of the likelihoods derived from the data, and in particular does not update our knowledge of the inputs to take account of the likelihoods.

This induced or MC distribution for  $\phi$  can be used to determine a 90% credible interval for the 95<sup>th</sup> percentile of  $Cs$ . Similarly, the posterior sample can be used to develop a Bayesian approach 90% credible interval for the 95<sup>th</sup> percentile of  $Cs$ .

Figure 3 represents a comparison of the estimates of the 95<sup>th</sup> percentile for  $C_s$  that would be obtained using point estimate, Monte Carlo and Bayesian approaches. The point estimate for soil concentration of PCB is based on the 95<sup>th</sup> percentiles of  $Vd$  and the observed air data, and the 5<sup>th</sup> percentiles for  $b$ ,  $\rho$  and  $D$ .

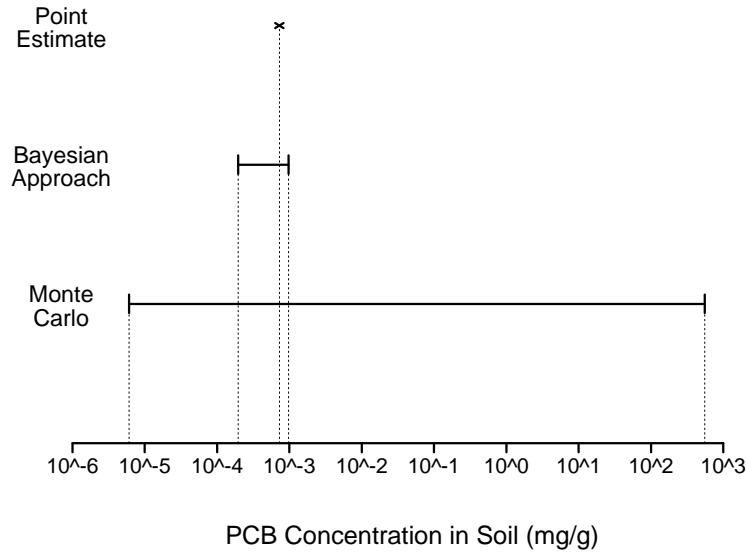


Figure 3: A point estimate of the 95<sup>th</sup> percentile of PCB concentration in soil as compared to 90% intervals for this percentile based on the Monte Carlo and Bayesian approaches.

The Bayesian interval is much narrower than the Monte Carlo one, reflecting the reduction in uncertainty due to the update of prior information by the likelihoods. We note that the prior distributions chosen for some inputs were diffuse and this causes the MC interval to be large. The point estimate of the 95<sup>th</sup> percentile of soil PCB concentration is  $7.3 \times 10^{-4} \text{ mg/g}$  while the Bayesian approach would estimate this to be  $9.7 \times 10^{-4} \text{ mg/g}$  (using the upper endpoint of the interval).

## 4 Discussion

The Bayesian approach presented is a method for dealing with uncertainty in inputs and outputs of deterministic models when data on the inputs and/or the outputs is available. Draper, Pereira, et al. (1999) presented a Bayesian method for uncertainty analysis with an application to risk assessment at a waste incineration site. In their application they had no data on which to base likelihoods or

update the prior information. Figure 3 illustrated the reduction in uncertainty arising from the use of likelihoods in our application.

The method gives insight into the behavior of the model at this site, as exhibited by the posterior distribution for deposition velocity which is consistent with little or no PCB adhering to fine particles.

In this application we sampled from the prior on inputs,  $p(\theta)$ , under an assumption of independence. If inputs to a model are correlated *a priori*, sampling can be adapted to account for this. However, prior correlations should not be confused with the expectation that the data will induce correlations between inputs. Our approach often yields high correlations between inputs *a posteriori*, even when their prior distributions are independent. Two examples of such are given in Figure 4. The contours represent the region covered by approximately 97% of the sample from the joint priors for;  $\ln(Vd)$  and  $\ln(\sigma_{\ln(Ca)})$ , and  $\rho$  and  $\ln(\mu_{\ln(Ca)})$ . No *a priori* correlation was assumed in this sampling. Superimposed are two-dimensional histograms of the posterior sample with darker shading indicating regions of higher density. We see correlation induced by the model and observed data. Priors based on independence will typically be more spread out than dependent priors, and will tend to cover the area covered by dependent priors fairly well. Thus it could be argued that prior independence provides a form of prior robustness, regardless of the extent to which it is scientifically justified.

We note that SIR is only one of the possible ways to generate a sample from a posterior distribution. Other methods include Markov chain Monte Carlo, and this could be used in principle to simulate from the posterior distributions here. However, posterior distributions in this kind of problem are often highly dependent, often being concentrated close to a submanifold or ridge in the high-dimensional space. Thus MCMC output will tend to be highly correlated, unlike our method, which yields independent samples. Designing a successful MCMC algorithm for the present application is an extremely delicate problem, and current generic MCMC methods are unlikely to do well, or even to be feasible.

In our work, we have taken account of prior information about inputs, but often in applications there is also prior information about outputs, which could also be expressed as a prior on outputs. If there is a prior on model output in addition to a likelihood, then the method of Bayesian melding (Poole and Raftery 2000) can be used to incorporate this extra source of information.

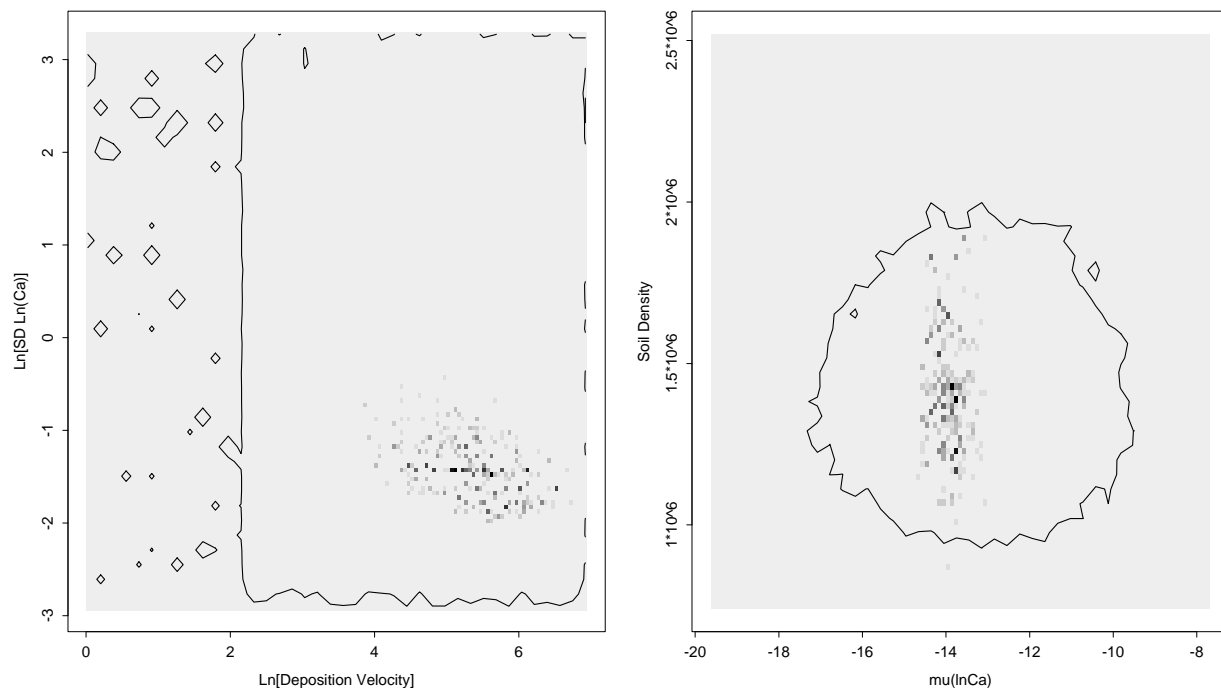


Figure 4: Grid-based contours represent the space covered by the sample from the joint prior distribution of  $(\ln(Vd), \ln(\sigma_{\ln(Ca)}))$  and  $(\mu_{\ln(Ca)}, \rho)$ . The contour contains approximately 97% of the non-zero mass grid points. A two-dimensional histogram of the SIR sample from the posterior distribution is superimposed. Darker shading indicates a higher density of sample values in that grid point.

## Acknowledgements

This research was supported by the National Research Center for Statistics and the Environment.

## References

- Bailey, W. H. (1997). Probabilistic approach to deriving risk-based exposure guidelines: Application to extremely low frequency magnetic fields. *Radiation Protection Dosimetry* 72(4), 327–336.
- Cullen, A. (1995). The sensitivity of probabilistic risk assessment results to alternative model structures: A case study of municipal waste incineration. *Journal of Air and Waste Management Association* 45, 538–546.



- Cullen, A. (2000). A comparison of measured and predicted contaminant concentration assuming simple compartmental modeling. *Environmental Science and Technology*. Submitted.
- Cullen, A. et al. (1996). Influence of harbor contamination on the level and composition of polychlorinated biphenyls in produce in Greater New Bedford, Massachusetts. *Environmental Science and Technology* 30(5), 1581–1588.
- Cullen, A. and H. Frey (1999). *Probabilistic techniques in exposure assessment: A handbook for addressing variability and uncertainty in models and inputs*. Plenum Publishing Corp.
- Draper, D., A. Pereira, et al. (1999). Scenario and parametric uncertainty in GESAMAC: A methodological study in nuclear waste disposal risk assessment. *Computer Physics Communications* 117, 142–155.
- Falconer, R. and T. Bidleman (1994). Vapor pressures and predicted particle/gas distributions of polychlorinated biphenyl congeners as functions of temperature and ortho-chlorine substitution. *Atmospheric Environment* 28(3), 547–554.
- Faustman, E. and G. Omenn (1996). *Casarett and Doull's toxicology; The basic science of poisons* (fifth ed.), Chapter 4, pp. 75–88. McGraw-Hill. New York, NY.
- Fries, G. and D. Paustenbach (1990). Evaluation of potential transmission of 2,3,7,8-tetrachlorodibenzo-p-dioxin contaminated incinerator emissions to humans via foods. *Journal of Toxicology and Environmental Health* 29, 1–43.
- Kass, R. and L. Wasserman (1995). A reference Bayesian test for nested hypotheses and its relationship to the Schwarz criterion. *Journal of the American Statistical Association* 90, 928–934.
- Morgan, M.G. Henrion, M. et al. (1985). Uncertainty in risk assessment. *Environmental Science and Technology* 19(8), 662–667.
- Ott, W. (1990). A physical explanation of the log-normality of pollutant concentrations. *Journal of Air and Waste Management Association* 14, 1378–1383.
- Poole, D. and A. Raftery (2000, Sept). Inference for deterministic simulation models: the Bayesian Melding approach. *Journal of the American Statistical Association* 95(451).
- Raftery, A. (1999, February). Bayes factors and BIC - Comment on “A critique of the Bayesian information criterion for model selection”. *Sociological Methods and Research* 27(3), 411–427.

- Rubin, D. (1988). Using the SIR algorithm to simulate posterior distributions. *Bayesian Statistics 3*, 395–402.
- Sehmel, G. (1980). Particle and gaseous dry deposition: A review. *Atmospheric Environment 14*, 983–1011.
- Steinberg, L., K. Reckhow, et al. (1995). A Bayesian model for the fate and transport of polychlorinated biphenyl in the upper hudson river. Technical Report 37, National Institute of Statistical Sciences.
- Taylor, A. (1992). *Addressing uncertainty in the estimation of environmental exposure and cancer potency*. Ph. D. thesis, Harvard School of Public Health, Boston, MA.
- US EPA (1997a). IRIS (Integrated Risk Information System): Polychlorinated biphenyls (PCBs). Internet.
- US EPA (1997b, January 29). Proposed policy for use of Monte Carlo analysis in Agency risk assessment. Memorandum of William P Wood, Executive Director Risk Assessment Forum to Dorothy E Patton, Executive Director of Science Policy Council (8104).
- Vorhees, D., A. Cullen, et al. (1997). Exposure to polychlorinated biphenyls in residential indoor air and outdoor air near a Superfund site. *Environmental Science and Technology 31*, 3612–3618.
- Vorhees, D., A. Cullen, et al. (1999). Exposure to polychlorinated biphenyls in house dust and yard soil near a Superfund site. *Environmental Science and Technology 33*, 2151–2156.
- Whitby, K. (1978). The physical characteristics of sulfur aerosols. *Atmospheric Environment 12*, 135–159.